The relative growth of optical and radio quasars in SDSS

Francesco Shankar,[1]★ Gregory R. Sivakoff,[2] Marianne Vestergaard[3,5] and Xinyu Dai[4]

[1]*Max-Planck-Institüt für Astrophysik, Karl-Schwarzschild-Str. 1, D-85748, Garching, Germany*
[2]*Department of Astronomy, University of Virginia, Charlottesville, VA 22904-4325, USA*
[3]*Dark Cosmology Centre Niels Bohr Institute at Copenhagen University Juliane Maries Vej 30 DK-2100 Copenhagen O, Denmark*
[4]*Astronomy Department, University of Michigan, Ann Arbor, MI 48109, USA*
[5]*Steward Observatory 933 N Cherry Avenue Tucson, AZ 85718, USA*

ABSTRACT

We cross-correlate the Sloan Digital Sky Survey Data Release 3 quasar sample with Faint Images of the Radio Sky at Twenty centimetres (FIRST) and the Vestergaard et al. black hole (BH) mass sample to compare the mean accretion histories of optical and radio quasars. We find significant statistical evidence that radio quasars have a higher mean Eddington ratio λ at $z > 2$ with respect to optical quasars, while the situation is clearly reverse at $z < 1$. At $z > 2$, radio quasars happen to be less massive than optical quasars; however, as redshift decreases radio quasars appear in increasingly more massive BHs with respect to optical quasars. These two trends imply that radio sources are not a mere random subsample of optical quasars. No clear correlation between radio activity and BH mass and/or accretion rate is evident from our data, pointing to other BH properties, possibly the spin, as the driver of radio activity. We have checked that our main results do not depend on any evident bias. We perform detailed modelling of reasonable accretion histories for optical and radio quasars, finding that radio quasars grows by a factor of a few, at the most, since $z \sim 4$. The comparison between the predicted mass function of active radio quasars and the observed optical luminosity function of radio quasars, implies a significantly lower probability for lower mass BHs to be radio loud at all epochs, in agreement with what is observed in the local universe.

Key words: galaxies: active – galaxies: jets – quasars: general.

1 INTRODUCTION

Jiang et al. (2007) have recently determined that ∼10 per cent of optically selected quasars in the Sloan Digital Sky Survey (SDSS) are radio-loud, here meaning that they have enough radio power to be detected in the Faint Images of the Radio Sky at Twenty centimetres (FIRST; Becker, White & Helfand 1995) survey. This fraction seems to depend on luminosity and redshift; however, it is still unclear why and how only a minority of active galactic nuclei (AGNs) show signatures of powerful radio emission. The simplest scenario usually invoked is the evolutionary one (e.g. Rees 1984), where all AGNs experience a brief radio-loud phase. Within this interpretation, the radio phase of quasars must therefore occur on an overlapping time-scale much shorter than the optical phase, to explain the small fraction of radio-loud sources within optical samples. Bird, Martini & Kaiser (2008) by matching analytical model predictions to observed source sizes, have recently found the radio-jet time-scales to be on the order of ∼10^7 yr, significantly shorter than the optical time-scale for quasars, constrained to be

$\gtrsim 5 \times 10^7$ yr from demographic arguments (e.g. Marconi et al. 2004; Shankar et al. 2004; Yu & Lu 2008; Shankar, Weinberg & Miralda-Escudé 2009c). However, the Bird et al. findings may only probe a single phase of radio-loudness, while AGNs may undergo several of these events. Although still limited by the poor knowledge of a comprehensive census for the radio-loud AGN population, preliminary demographic studies point towards longer cumulative time-scales for the radio phase (e.g. Merloni & Heinz 2008; Shankar et al. 2008c).

Theoretically, the origin of AGN radio-loudness still constitutes an open issue. Empirically, still no clear, strong correlation between radio-loudness and any black hole (BH) property, such as mass, luminosity, Eddington ratio or spin has yet been found. There is tentative evidence suggesting that the formation of a relativistic jet or a fast wind (e.g. Blundell & Kuncic 2007) sustaining the radio emission is tightly related to the mass of the central BH (e.g. Laor 2000). Best et al. (2005) constructed a large sample of radio-loud AGNs cross-correlating FIRST, SDSS and the National Radio Astronomy Observatory Very Large Array Sky Survey (NVSS; Condon et al. 1998), finding that the fraction of radio-loud AGNs is a strong increasing function of the central BH mass and galactic stellar mass (M_{STAR}).

★E-mail: shankar@mpa-garching.mpg.de

Although BH mass might indeed represent an important aspect regulating radio-loudness, it cannot be the only key driver. The wide scatter observed between radio and optical luminosities (e.g. Cirasuolo et al. 2003), and radio power and Eddington ratios (e.g. Marchesini, Celotti & Ferrarese 2004; Sikora, Stawarz & Lasota 2007), for example, suggest that other parameters such as the mass accretion rate on to the BH and possibly its spin could also play a major role in determining when a galaxy becomes radio-loud (e.g. Blandford 1999; Sikora et al. 2007; Ghisellini & Tavecchio 2008). Theoretical arguments such as those by Blandford & Znajek (1977), also propose that jets are powered by the extraction of energy already accumulated in a rotating BH. On the other hand, the efficiency of the energy extraction from the spinning BH may not provide the necessary power for energizing the very luminous sources. Alternative models (e.g. Livio, Ogilvie & Pringle 1999; Cavaliere & D'Elia 2002) have therefore proposed that a significant fraction of the jet or wind kinetic power must be directly linked to the rest-mass energy of the currently accreting matter, thus suggesting some possible link also between radio power and Eddington ratio (e.g. Sikora et al. 2007; Ghisellini & Tavecchio 2008, and references therein).

Some phenomenological constraints on the nature of jets come from the observed correlations between radio and kinetic powers, the latter empirically measured by tracing the integrated pdV work done by radio AGNs in excavating the cavities observed in the hot gaseous medium around them (e.g. Rawlings & Saunders 1991; Willott et al. 1999; Allen et al. 2006; Hardcastle, Evans & Croston 2007; Merloni & Heinz 2008). Knowing the exact kinetic power in AGN jets can provide important clues on the jet composition, on the origin of the synchrotron emission, on the relative contributions of positrons, protons, and Poynting flux to the overall energy budget (e.g. Blandford & Payne 1982; Meisenheimer 2003; Lazarian 2006), and on the nature of the jet collimation up to Mpc scales. Shankar et al. (2008c) constrained the fraction g_k of bolometric luminosity turned into kinetic power, by using an optically selected sample for which both the optical and the radio luminosity functions were determined. Given the empirical correlations optical and radio luminosities have with bolometric and kinetic powers, respectively, they converted the optical luminosity function into a radio one. The match with the radio luminosity function independently determined for the same sample, yielded $g_k \sim 0.10$, with a significant scatter around the mean, in line with several independent studies (e.g. Körding, Jester & Fender 2008; Merloni & Heinz 2008; Cattaneo & Best 2009). The levels of kinetic power derived from these works are in agreement with the amount of kinetic feedback required in theoretical studies of massive galaxies (e.g. Granato et al. 2004; Croton et al. 2006; Cavaliere & Lapi 2008). Also, constraining the kinetic efficiency g_k can provide useful constraints on the duty cycle of radio sources and, in turn, set constraints on the origin of radio-loudness (see Cattaneo & Best 2009; Shankar et al. 2008c).

In addition, understanding the main physical processes that make an AGN radio-loud is of key importance for assessing the true role AGNs and supermassive BHs played in the evolution of galaxies. It has now been proven, in fact, that most, if not all, local galaxies have a BH at their centre, the mass of which is tightly correlated with the velocity dispersion σ and other bulk properties of the host galaxy (e.g. Ferrarese & Merritt 2000; Gebhardt et al. 2000; Marconi & Hunt 2003; Graham 2007). Liu & Jiang (2006) found significant evidence that radio-loud AGNs follow a different $M_{BH}-\sigma$ relation than radio-quiet ones, even after accounting for different selection effects. A similar offset has been observed for the $M_{BH}-M_{STAR}$ relation (Kim et al. 2008).

Semi-analytic models of galaxy formation have grown BHs within galaxies (e.g. Granato et al. 2004, 2006; Croton et al. 2006; Monaco, Fontanot & Taffoni 2007; Marulli et al. 2008) and showed that the energetic radiative and kinetic back reactions of AGNs (e.g. Monaco & Fontanot 2005; Sazonov et al. 2005; Churazov et al. 2005; Merloni & Heinz 2008; Ciotti, Ostriker & Proga 2009, and references therein) can solve the overcooling problem in massive systems and contemporarily settle the local relations between BH mass and galaxy properties. However, numerical hydro simulations and some theoretical arguments seem to limit the actual need for AGN feedback, at least in some regimes (e.g. Miralda-Escudé & Kollmeier 2005; Dekel et al. 2009; Keres et al. 2009).

The nature of AGN feedback is still unclear. Although there are theoretical (e.g. Murray et al. 1995; Granato et al. 2004; Vittorini, Shankar & Cavaliere 2005; Granato et al. 2006; Lapi et al. 2006; Shankar et al. 2006; Menci et al. 2008) and empirical arguments (e.g. Ganguly et al. 2007; Dai, Shankar & Sivakoff 2008; Shankar, Dai & Sivakoff 2008b) in favour of an AGN feedback driven by winds arising from the accretion disc around the central BH, other models (e.g. Saxton et al. 2005; Silk 2005; Pipino, Silk & Matteucci 2009) propose that it is instead a *jet* that is the actual driver for AGN feedback. A jet can propagate through an inhomogeneous interstellar medium, forming an expanding cocoon. The interaction of the outflow with the surrounding protogalactic gas at first stimulates star formation on a short time-scale, 10^7 yr or less, but will eventually expel much of the gas in a wind.

It is therefore clear that understanding AGN radio-loudness from first principles, can on one hand reveal interesting features of BH physics, and on the other hand provide constraints on models for AGN feedback related to the cosmological co-evolution of BHs and galaxies. In this paper, we use the quasar sample used in Shankar et al. (2008b), which is the result of the cross-correlation between the SDSS Data Release 3 (DR3) quasar catalogue and FIRST. By combining it with the BH mass measurements and bolometric luminosities presented in Vestergaard et al. (2008), we were able to compare accretion properties of large samples of optical and radio quasars. Although optically selected radio quasars may only be a partial representation of the overall radio population, they have the enormous advantage of providing us with the knowledge of fundamental quantities such as the bolometric luminosity and BH mass. We find significant differences in the accretion histories of radio and optical quasars at fixed BH mass and redshift already since $z \sim 4$, supporting a clear distinction between these two populations. We do not find any clear correlation between radio-loudness and BH mass and/or accretion rate. These results therefore may support a scenario in which radio quasars are BHs with environments and/or intrinsic properties (such as the spin) *different* from the optical quasars. In separate papers (Shankar et al. 2009a; Sivakoff et al., in preparation), we will investigate further results when distinguishing among Fanaroff & Riley (1974, FR) sources and broad absorption line quasars. Our aim in these papers is to constrain the differences in accretion histories for different families of AGNs, thus providing useful empirical constraints for theoretical models.

This paper is organized as follows. In Section 2, we describe the data sets used for the cross-correlations and BH mass estimates. In Section 3, we provide our results on the Eddington ratio, BH mass and redshift distributions of optical and radio quasars. In Section 4, we discuss our findings, in reference to previous works and give our conclusions in Section 5. Throughout this paper, we use the cosmological parameters $\Omega_m = 0.30$, $\Omega_\Lambda = 0.70$ and $H_0 = 70 \text{ km s}^{-1} \text{ Mpc}^{-1}$.

2 DATA

We adopt the SDSS DR3 quasar catalogue by Schneider et al. (2005) as the basis for our analysis. The data for this sample were taken in five broad optical bands (*ugriz*) over about $10\,000$ deg^2 of the high Galactic latitude sky. The majority of quasars were selected for spectroscopic follow-up by SDSS based on their optical photometry. In particular, most quasar candidates were selected by their location in the low-redshift ($z \lesssim 3$) *ugri* colour cube with its *i*-magnitude limit of 19.1. A second higher redshift *griz* colour cube was also used with a fainter *i*-magnitude limit of 20.2.

The DR3 quasar catalogue by Schneider et al. (2005) also provides the radio flux density for those sources which have a counterpart within 2 arcsec in the FIRST catalogue (Becker et al. 1995). According to Schneider et al. (2005), while only a small minority of FIRST-SDSS matches are chance superpositions, a significant fraction of the DR3 sources are extended radio sources. This can lead to slightly larger offsets between SDSS and FIRST positions, as well as multiple radio components. Furthermore, radio lobes may be more strongly offset from the central optical source. As discussed in Shankar et al. (2008b), we built a full FIRST-SDSS cross-correlation catalogue, containing all the detected radio components within 30 arcsec of a optical quasar. From this catalogue, we define a radio quasar as any SDSS quasar with either a single FIRST component within 5 arcsec (FRI) or multiple FIRST components within 30 arcsec (FRII). While here we are mainly interested in identifying all the possible radio matches within the optical sample, in a separate paper (Shankar et al. 2009a), we will focus on the differences in the intrinsic properties of compact and extended radio sources. The remaining SDSS quasars that overlap with FIRST are defined as an optical quasar. In this paper, the radio sample is restricted to radio quasars whose sum of the integrated flux density in FIRST f_{int} is above 3 mJy.

We remind the reader here that FIRST efficiently identifies radio matches to optically selected quasars. By cross-correlating SDSS with the large radio NRAO VLA Sky Survey Condon et al. (1998), Jiang et al. (2007) found in fact that only ∼6 per cent of the matched quasars were not detected by FIRST. In this paper, we cross-correlate our sample with the one worked by Vestergaard et al. (2008). The latter estimated the mass function of active BHs using the quasar sample by Richards et al. (2006a) with a well-understood selection function. The reader is referred to Richards et al. (2006a) for details on this sample and its selection. To estimate the mass of the central BH in each quasar, Vestergaard et al. (2008) measured the widths of each of the Hβ, Mg II and C IV emission lines, and the monochromatic nuclear continuum luminosity near these emission lines, with each spectrum corrected for Galactic reddening and extinction. When a particular quasar had two emission lines for which it was possible to determine a BH mass, the final mass estimate was taken to be the variance weighted average of the individual emission line based mass estimates. The continuum components were modelled using a nuclear power-law continuum, an optical–ultraviolet iron line spectrum, a Balmer continuum, and a host galaxy spectrum. The monochromatic nuclear continuum luminosities near the emission lines were used to calculate the bolometric luminosity for the quasar. The continuum components were subtracted and the emission lines were then modelled with multiple Gaussian functions so to obtain smooth representations of the data. All Mg II and C IV profiles with strong absorption, as identified by visual inspection of the quasar spectra in the Trump et al. (2006) catalogue and of the quasars with redshifts between 1.4, when C IV enters the observing window, and 1.7, were discarded by Vestergaard et al. (2008) from

further analysis. Of the $15\,180$ quasars on which the DR3 quasar luminosity function is based, BH mass estimates were possible for $14\,434$ quasars (95 per cent).

The bolometric luminosities are based on the fitted nuclear power-law continuum level extrapolated to 4400 Å, L_λ, obtained from the spectral decomposition. The λL_λ (4400 Å) values are scaled by a bolometric correction factor of $9.20(\pm0.24)$, determined from the data base of Richards et al. (2006b). We checked that results do not change when adopting different wavelengths at which luminosities were estimated.

3 RESULTS

In Fig. 1, we show the sample of optical and radio quasars in slices of the redshift-bolometric luminosity-BH mass plane. The contours levels delineate the regions containing 25, 50, 75 and 95 per cent of the optical quasars; individual solid black dots represent the remaining 5 per cent. The red squares individually show the radio quasars. It is clear from this figure that the radio and optical samples are well mixed at all luminosities and redshifts, and there is no apparent selective segregation between the two types of AGNs. The lower right-hand panel of Fig. 1 shows that the bulk of the optical and radio quasars are strong accretors with Eddington ratios[1] within $0.1 < \lambda < 1$, in line with several independent studies (e.g. Vestergaard 2004; Kollmeier et al. 2006; Netzer et al. 2007; Shen et al. 2008). The super-Eddington accretors are a minority (e.g. McLure & Dunlop 2004), while there is a non-negligible fraction of sources radiating at significantly sub-Eddington regimes. To further develop the comparison between optical and radio sources, we present a more detailed study in the following section, dividing the optical and radio samples in bins of redshift, BH mass and Eddington ratios.

3.1 Eddington ratios

Fig. 2 shows normalized distributions[2] of Eddington ratios for active BHs in different redshift bins, as labelled. The left-hand panel considers only BHs with mass within the range $6.59 \lesssim \log M_{BH}/M_\odot \lesssim 9.0$, while the right-hand panel considers only the subsamples of more massive BHs with mass $\log M_{BH}/M_\odot > 9$. In both panels, the solid and dotted lines refer to radio and optical quasars, respectively. We find that the distributions of radio quasars are clearly skewed towards higher values of λ at redshifts $z > 2$. The distributions get closer at intermediate redshifts $1 < z < 2$, while radio quasars shift towards lower Eddington ratios at lower redshifts. A similar, and even more marked behaviour, is present in the λ-distributions of the more massive BHs, plotted in the right-hand panel of Fig. 2. Radio quasars accrete at significantly higher Eddington ratios at $z > 2$ and then later in time move towards lower and lower λ s faster than optical quasars. We have checked that these results do not depend on the exact choice of the redshift bins in which we divide the samples, as long as a significant number of sources for both samples are present in each bin.

---

[1] We define as Eddington ratio the quantity $\lambda = L/L_{Edd}$, with L the bolometric luminosity and $L_{Edd} = 1.26 \times 10^{38}\,(M_{BH}/M_\odot)$ erg s^{-1}.

[2] Throughout the paper, we indicate normalized distributions with the letter f in the figures.
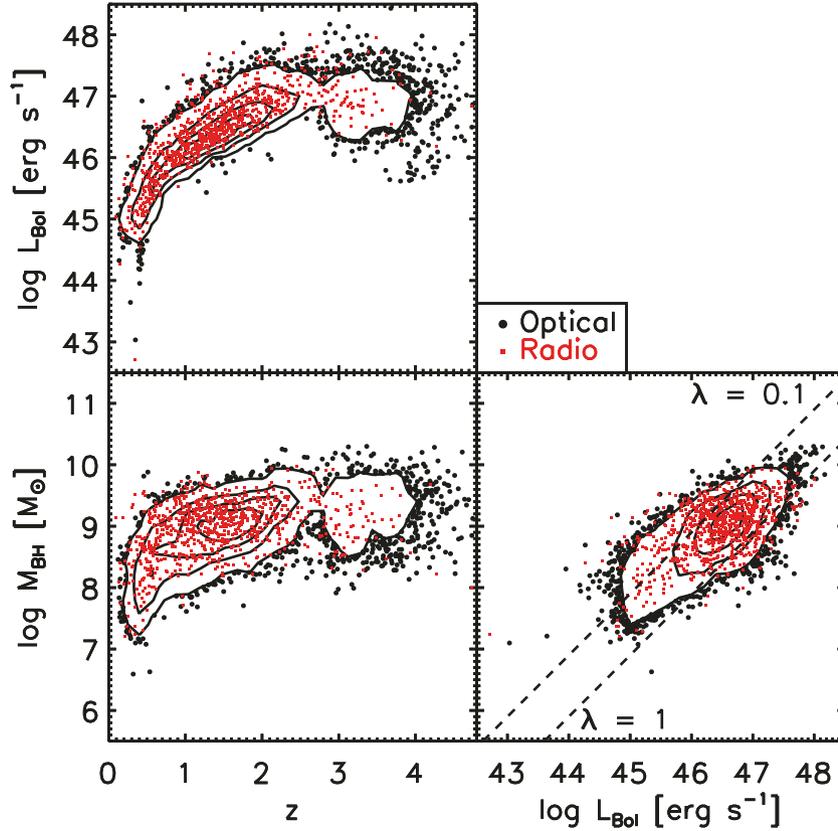
Figure 1. Overall distributions of bolometric luminosities, BH masses and redshifts for the samples of SDSS quasars with and without FIRST counterparts, radio and optical quasars, respectively, used in this paper. The solid contours delineate the regions containing 25, 50, 75 and 95 per cent of the optical sample. The black dots individually indicate the remaining 5 per cent of optical quasars. All radio quasars are shown by the red squares. The optical and radio quasars cover similar areas with no clear systematic offsets between the distributions. The dashed lines in the lower right panel show the locus of points in the $M_{BH} - L$ plane with $\lambda = 0.1$ and 1, as labelled ($\lambda = L/L_{Edd}$).
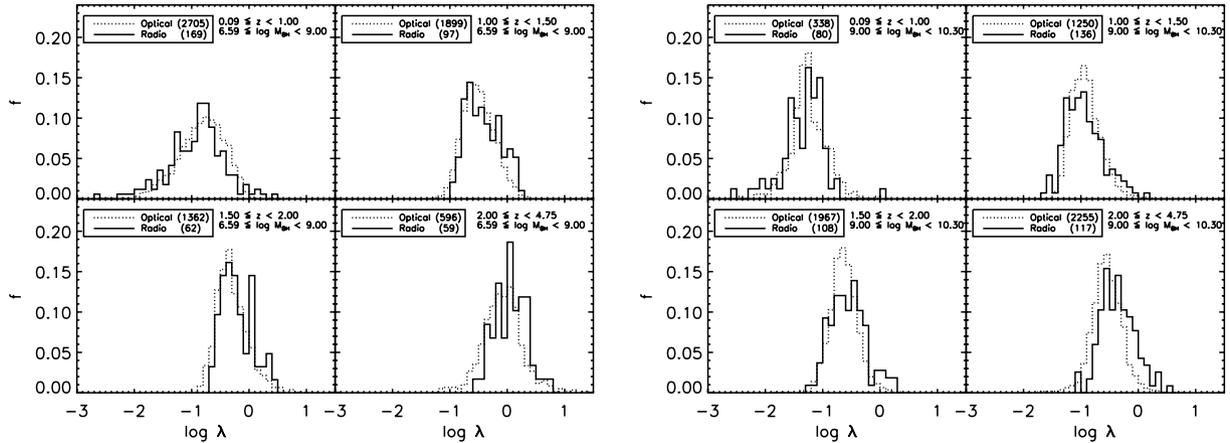
Figure 2. Left-hand panel: normalized distribution of Eddington ratios for active BHs with mass in the range $6.59 \lesssim \log M_{BH}/M_{\odot} \lesssim 9.0$ and in different redshift bins, as labelled. Right-hand panel: normalized distributions of Eddington ratios for active BHs with mass in the range $9.00 \lesssim \log M_{BH}/M_{\odot} \lesssim 10.30$ and in different redshift bins, as labelled. Solid lines refer to radio quasars alone, while dotted lines refer to optical quasars only. Irrespective of the BH mass interval considered, the Eddington ratio distributions of radio quasars are skewed towards higher values of λ at higher redshifts. In parenthesis, we list the number of quasars in each sample.

3.2 Black hole masses

Fig. 3 shows the normalized distributions of BH mass for optical and radio quasars (dotted and solid lines, respectively) in the same four redshift bins considered in Fig. 2. The left-hand panel shows the distribution of only the 'fading' quasars, i.e. those shining at low

Eddington ratios, in the range $-2.6 \leq \log \lambda < -0.6$. We find that, at all times, the radio quasars have a BH mass distribution peaked at higher masses than optical quasars, on an average. The right-hand panel shows instead that the former trend is not apparent in highly accreting quasars with $-0.6 \leq \log \lambda < 1.3$. Radio quasars exhibit a slight tendency to have *lower* BH masses than optical sources at
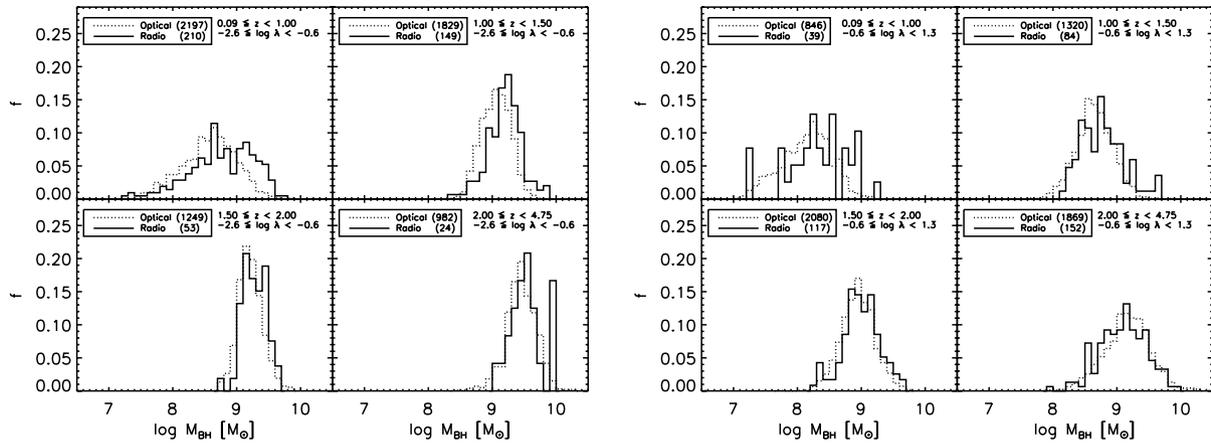
Figure 3. Left-hand panel: normalized distributions of BH mass for active BHs with Eddington ratio in the range $-2.6 \le \log \lambda < -0.6$. Right-hand panel: normalized distributions of BH mass for active BHs with Eddington ratio in the range $0.6 \le \log \lambda < 1.3$. In both panels dotted lines refer to optical quasars while solid lines to radio ones. While for sources accreting at low Eddington ratios radio quasars always have higher BH masses, on average, there is no clear distinction in the BH mass distributions for radio and optical quasars accreting at higher Eddington ratios. In parenthesis, we list the number of quasars in each sample.
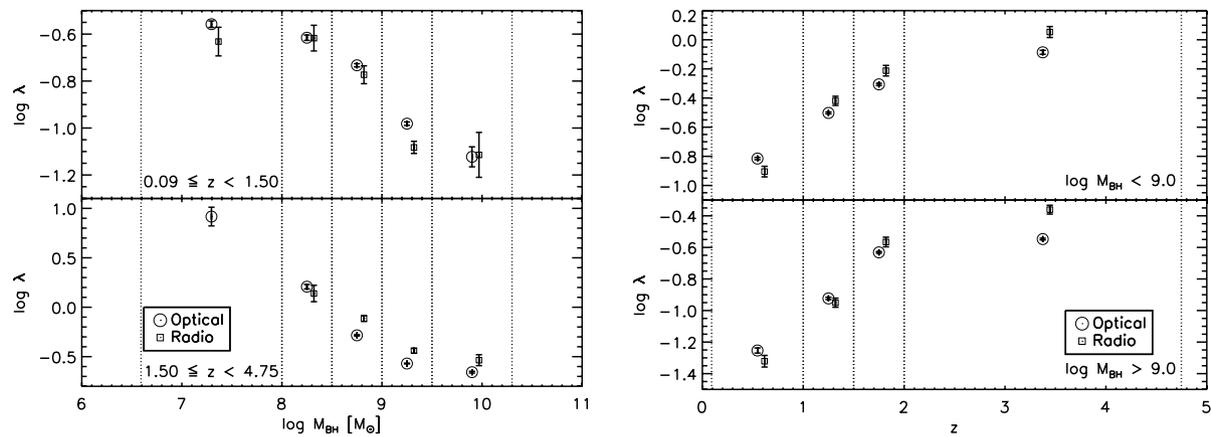
Figure 4. Left-hand panel: mean Eddington ratio as a function of BH mass for sources at $z < 1.5$ (upper plot) and at $z \ge 1.5$ (lower plot). Right-hand panel: mean Eddington ratio as a function of redshift for BHs with mass $\log M_{BH}/M_{\odot} < 9.0$ (upper panel) and $\log M_{BH}/M_{\odot} \ge 9.0$ (lower panel). In both panels, radio and optical quasars are shown with squares and circles, respectively. With respect to optical quasars, massive radio quasars tend to have higher Eddington ratios at higher redshifts and lower or comparable Eddington ratios at lower redshifts. Also, radio quasars tend to have higher Eddington ratios at $z \gtrsim 1.5$, and lower Eddington ratios at lower redshifts. Here and in the following figures, the vertical dotted lines mark the redshift intervals in which the sample was divided, and the results do not depend on the exact choice of such intervals.

$z > 2$, comparable BH masses at intermediate redshifts $1.5 < z < 2$, and higher BH masses at lower redshifts. This shows that radio quasars in general are not a random subsample of optical quasars, and have a specific, different cosmological accretion history than optical quasars.

3.3 Comparing the mean values of the distributions

In the previous sections, we showed that interesting differences arise when comparing the Eddington ratio and BH mass distributions for optical and radio sources. The distributions we find in each sample considered are always broad, due to a combination of intrinsic scatter and measurement errors (e.g. Shen et al. 2008). It is therefore worth comparing only the mean values of the distributions.[3] Given

[3] We stress that although mean and median quantities do not often coincide in our sample, our results on the systematic differences between the properties characterizing optical and radio sources are robust against using either of the two.

the large statistics in our sample, the mean values are well defined and the errors on the means are small enough to provide significant constraints. In this section, we therefore summarize our results by comparing the mean values of the distributions of optical and radio quasars. We plot these comparisons in four bins of redshift and BH mass chosen in a way to yield a similar number of sources separately for optical and radio quasars, as was done for the previous figures. However, the results do not depend on how we decide to bin the data. For example, choosing narrower bins actually enhances the differences between optical and radio quasars.

With respect to optical quasars, radio quasars tend to have higher Eddington ratios at redshifts $z > 1.5$ while they accrete at lower, or at most comparable, rates at lower redshifts. The right-hand panel of Fig. 4 shows that the mean λ of radio quasars (squares) is significantly higher than the mean λ of optical quasars at $z > 1.5$, for BHs with mass below (upper plot) and above (lower plot) $\log M_{BH}/M_{\odot} = 9.0$. At lower redshifts, all quasars progressively decrease their mean Eddington ratio, but the mean λ associated with radio quasars decreases faster, and eventually becomes lower, than

the one associated with optical quasars. Note that high mass radio quasars with $\log M_{BH}/M_\odot > 9$ 'cross' the optical mean λ around redshift $z \sim 1.5$, while lower mass radio quasars cross the optical boundary at later times, around $z \sim 1$.

The subsample of sources with BH masses above $\log M_{BH}/M_\odot = 9$ is particularly meaningful. In fact, this subsample suffers from flux-limited effects much less than the total sample (cf. Fig. 1), thus further supporting the evidence that the differences between optical and radio quasars are not induced by SDSS selection effects. To be even more conservative, when selecting the sources with $\log M_{BH}/M_\odot > 9$, $\lambda > -0.6$, and $1 < z < 2$, to ensure full detectability above the SDSS flux limits, we find that optical and radio sources still differ in their mean λ at the 3.3σ significance level.

Taken at face value, the data seem to also support a decreasing λ with decreasing redshift, for both optical and radio sources, in line with previous studies (e.g. McLure & Dunlop 2004; Vestergaard 2004; Netzer & Trakhtenbrot 2007). When restricting the analysis to the subsample of massive BHs with $\log M_{BH}/M_\odot > 9$, we still find significant evidence for a decrease in λ (2.6σ), although the amplitude of the drop is smaller. A decreasing λ with decreasing z is not surprising, given that locally the median Eddington ratio of all BHs is only a few per cent (Kauffmann & Heckman 2008), that is at least an order of magnitude lower than what is observed for luminous quasars at high redshifts (e.g. Vestergaard 2004; Kollmeier et al. 2006; Shen et al. 2008).

The left-hand panel of Fig. 4 shows instead significant evidence for a decrease in the mean Eddington ratio with increasing BH mass for all quasars regardless of radio properties. This trend seems to be independent of redshift, although at least part of the observed drop might depend on selection effects (see Shen et al. 2008). In physical terms, this behaviour would naturally arise if more massive BHs tend to accrete most of their mass at early times and then undergo a long, 'post-peak' descending phase characterized by lower and lower Eddington ratios (e.g. Granato et al. 2004; Fontanot et al. 2006; Hopkins & Hernquist 2009; Yu & Lu 2008; Ciotti et al. 2009 and references therein). Many groups claimed a decreasing Eddington ratio with increasing BH mass, using both brighter and fainter samples than ours (e.g. McLure & Dunlop 2004; Kollmeier et al. 2006; Netzer & Trakhtenbrot 2007; Shen et al. 2008; Dietrich et al. 2009). In particular, Hickox et al. (2009) recently presented

the Eddington ratio distributions of a sample of 585 AGNs at $0.25 < z < 0.8$, finding that radio AGNs, on average the most massive BHs in their sample, have a median λ much lower than AGNs identified in other bands, characterized by lower mass BHs.

The left-hand panel of Fig. 5 shows instead the mean BH mass in the optical and radio samples as a function of redshift for low and high accretors (upper and lower plots, respectively). While radio-loud, low accretors always have higher BH masses with respect to optical quasars, in the lower plot we see a tendency for radio quasars to have lower BH masses at $z > 2$ and a steady increase to higher masses at lower redshifts. Therefore, irrespective of how fast quasars are accreting, at late times radio quasars seem to always be associated with more massive systems, with the mass difference gradually decreasing with increasing redshifts. A similar result was also found by Metcalf & Magliocchetti (2006) using a homogeneous sample of $\sim$300 radio-loud quasars drawn from the FIRST and 2dF quasi-stellar object surveys in the range $0.3 < z < 3$. To check that these trends are not affected by flux-limit issues, in the right-hand panel of Fig. 5 we show the same plots for only the subsample of sources with BH mass above $\log M_{BH}/M_\odot = 9$, which fully confirms the trends derived for the full sample.

To evaluate the significance of our results, we performed a Student T-test (allowing for unequal variances) on the difference between the means of the distributions in each bin of redshift considered. The means and standard deviations of the distributions are computed from the biweight mean μ and biweight standard deviation σ (Hoaglin, Mosteller & Tukey 1983). Errors on this mean were estimated by reducing σ by $\sqrt{N}$, where N is the number of quasars in the distribution. Table 1 summarizes the differences in the mean λ-distributions of optical and radio sources, for each bin of redshift and BH mass considered so far. In the last column, we report the probability that optical and radio quasars have the same mean, as determined by the Student's T statistic P_T. It is evident that a clear pattern arises when comparing the λ-distributions of the two quasar populations. Irrespective of the BH mass bin considered, the mean Eddington ratio differs significantly at $z \gtrsim 2$ at the $\sim 3\sigma$ level (i.e. $P_T < 2.7 \times 10^{-3}$), getting more similar at moderate redshifts $1.5 \lesssim z \lesssim 2$, and differentiating again at lower redshift at a slightly lower, but still significant, 2σ level (i.e. $P_T < 4.6 \times 10^{-2}$). Table 2 shows that the difference in the median value of the M_{BH}-distributions become, on average, significantly more different when moving from
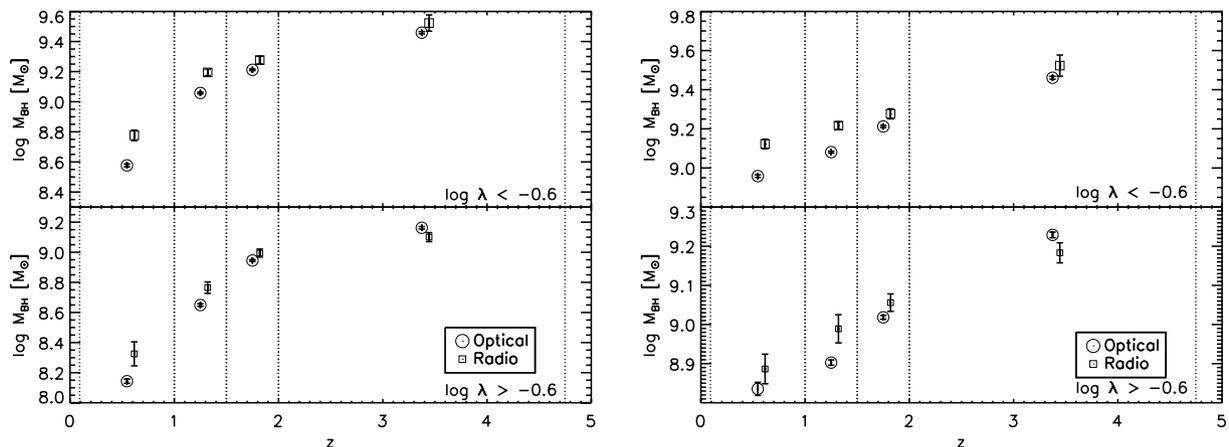
Figure 5. Left-hand panel: mean BH mass as a function of redshift for sources accreting with an Eddington ratio $\log \lambda < -0.6$ (upper plot) and $\log \lambda > -0.6$ (lower plot). Right-hand panel: same pattern as left-hand panel considering only the subsample of sources with BH mass higher than $10^{8.7}$ M$_\odot$, for which no strong luminosity bias should be present. In both panels, optical and radio sources are shown with circles and squares, respectively, as labelled. Radio sources with high λ have lower masses with respect to optical ones at $z > 1.5$, but have a tendency for higher BH masses at lower redshifts.

Table 1. Eddington ratio distributions of optical and radio quasars.

| | Ranges | | | Optical quasars (O) | | | Radio quasars (R) | | | |
Row	z	$\log M_{BH}$	N	$\mu(\log \lambda)$	$\sigma(\log \lambda)$	N	$\mu(\log \lambda)$	$\sigma(\log \lambda)$	$\mu_O - \mu_R$	P_T
1	[0.09,1.00)	[6.59, 9.00)	2705	-0.815 ± 0.008	0.40	169	-0.905 ± 0.036	0.47	0.089 ± 0.037	2.1E-02
2	[1.00,1.50)	[6.59, 9.00)	1899	-0.502 ± 0.006	0.28	97	-0.419 ± 0.031	0.31	-0.083 ± 0.032	9.0E-03
3	[1.50,2.00)	[6.59, 9.00)	1362	-0.306 ± 0.007	0.26	62	-0.212 ± 0.036	0.29	-0.094 ± 0.037	1.6E-02
4	[2.00,4.75)	[6.59, 9.00)	596	-0.086 ± 0.014	0.33	59	0.053 ± 0.038	0.29	-0.139 ± 0.040	8.8E-04
5	[0.09,1.00)	[9.00,10.30)	338	-1.253 ± 0.016	0.30	80	-1.321 ± 0.037	0.33	0.068 ± 0.040	7.5E-02
6	[1.00,1.50)	[9.00,10.30)	1250	-0.923 ± 0.007	0.25	136	-0.950 ± 0.029	0.34	0.027 ± 0.030	3.9E-01
7	[1.50,2.00)	[9.00,10.30)	1967	-0.632 ± 0.005	0.24	108	-0.566 ± 0.031	0.32	-0.066 ± 0.031	2.6E-02
8	[2.00,4.75)	[9.00,10.30)	2255	-0.547 ± 0.005	0.25	117	-0.361 ± 0.028	0.30	-0.186 ± 0.029	4.3E-10
9	[0.09,1.50)	[6.59, 8.00)	547	-0.558 ± 0.014	0.32	25	-0.632 ± 0.061	0.31	0.074 ± 0.063	3.5E-01
10	[0.09,1.50)	[8.00, 8.50)	1433	-0.615 ± 0.011	0.43	80	-0.617 ± 0.055	0.49	0.002 ± 0.056	9.9E-01
11	[0.09,1.50)	[8.50, 9.00)	2624	-0.733 ± 0.007	0.35	161	-0.773 ± 0.038	0.48	0.040 ± 0.039	2.4E-01
12	[0.09,1.50)	[9.00, 9.50)	1533	-0.981 ± 0.007	0.29	191	-1.082 ± 0.026	0.36	0.101 ± 0.027	6.4E-04
13	[0.09,1.50)	[9.50,10.30)	55	-1.123 ± 0.043	0.32	25	-1.114 ± 0.096	0.48	-0.008 ± 0.105	8.9E-01
14	[1.50,4.75)	[6.59, 8.00)	4	0.917 ± 0.095	0.19	1	$0.755 \pm \cdot$	.	.	.
15	[1.50,4.75)	[8.00, 8.50)	180	0.208 ± 0.023	0.31	13	0.139 ± 0.083	0.30	0.069 ± 0.086	3.8E-01
16	[1.50,4.75)	[8.50, 9.00)	1774	-0.284 ± 0.006	0.27	107	-0.114 ± 0.029	0.30	-0.170 ± 0.030	9.4E-08
17	[1.50,4.75)	[9.00, 9.50)	3389	-0.570 ± 0.004	0.25	182	-0.440 ± 0.024	0.32	-0.130 ± 0.024	7.4E-08
18	[1.50,4.75)	[9.50,10.30)	833	-0.657 ± 0.009	0.25	43	-0.536 ± 0.055	0.36	-0.121 ± 0.056	2.1E-02
19	[0.09,1.00)	[6.59, 9.00)	2705	-0.815 ± 0.008	0.40	169	-0.905 ± 0.036	0.47	0.089 ± 0.037	2.1E-02
20	[1.00,1.50)	[6.59, 9.00)	1899	-0.502 ± 0.006	0.28	97	-0.419 ± 0.031	0.31	-0.083 ± 0.032	9.0E-03
21	[1.50,2.00)	[6.59, 9.00)	1362	-0.306 ± 0.007	0.26	62	-0.212 ± 0.036	0.29	-0.094 ± 0.037	1.6E-02
22	[2.00,4.75)	[6.59, 9.00)	596	-0.086 ± 0.014	0.33	59	0.053 ± 0.038	0.29	-0.139 ± 0.040	8.8E-04
23	[0.09,1.00)	[9.00,10.30)	338	-1.253 ± 0.016	0.30	80	-1.321 ± 0.037	0.33	0.068 ± 0.040	7.5E-02
24	[1.00,1.50)	[9.00,10.30)	1250	-0.923 ± 0.007	0.25	136	-0.950 ± 0.029	0.34	0.027 ± 0.030	3.9E-01
25	[1.50,2.00)	[9.00,10.30)	1967	-0.632 ± 0.005	0.24	108	-0.566 ± 0.031	0.32	-0.066 ± 0.031	2.6E-02
26	[2.00,4.75)	[9.00,10.30)	2255	-0.547 ± 0.005	0.25	117	-0.361 ± 0.028	0.30	-0.186 ± 0.029	4.3E-10

Notes. For each specified range, this table lists the number of optical and radio quasars N, and the (biweight) mean μ and (biweight) standard deviation σ for distributions of the logarithm of the Eddington ratio. Both the difference of the means $\mu_O - \mu_R$ and the statistical chance the optical and radio quasars have the same mean as determined by the Student's T statistic P_T are listed.

Table 2. Black hole mass distributions of optical and radio quasars.

| | Ranges | | | Optical quasars (O) | | | Radio quasars (R) | | | |
Row	z	$\log \lambda$	N	$\mu(\log M_{BH})$	$\sigma(\log M_{BH})$	N	$\mu(\log M_{BH})$	$\sigma(\log M_{BH})$	$\mu_O - \mu_R$	P_T
1	[0.09,1.00)	[−2.7,−0.6)	2197	8.577 ± 0.009	0.43	210	8.776 ± 0.035	0.51	-0.199 ± 0.036	1.4E-07
2	[1.00,1.50)	[−2.7,−0.6)	1829	9.058 ± 0.005	0.23	149	9.194 ± 0.021	0.26	-0.137 ± 0.022	1.5E-08
3	[1.50,2.00)	[−2.7,−0.6)	1249	9.212 ± 0.005	0.19	53	9.276 ± 0.026	0.19	-0.064 ± 0.026	2.2E-02
4	[2.00,4.75)	[−2.7,−0.6)	982	9.459 ± 0.007	0.23	24	9.523 ± 0.054	0.27	-0.064 ± 0.055	1.9E-01
5	[0.09,1.00)	[−0.6, 1.4)	846	8.143 ± 0.014	0.40	39	8.325 ± 0.080	0.50	-0.182 ± 0.081	3.2E-02
6	[1.00,1.50)	[−0.6, 1.4)	1320	8.649 ± 0.008	0.29	84	8.765 ± 0.038	0.35	-0.116 ± 0.039	1.4E-03
7	[1.50,2.00)	[−0.6, 1.4)	2080	8.945 ± 0.006	0.26	117	8.994 ± 0.027	0.29	-0.049 ± 0.027	8.5E-02
8	[2.00,4.75)	[−0.6, 1.4)	1869	9.163 ± 0.008	0.36	152	9.100 ± 0.030	0.37	0.062 ± 0.031	3.4E-02
9[a]	[0.09,1.00)	[−2.7,−0.6)	869	8.958 ± 0.007	0.20	116	9.122 ± 0.024	0.26	-0.164 ± 0.025	2.8E-09
10[a]	[1.00,1.50)	[−2.7,−0.6)	1723	9.081 ± 0.005	0.21	142	9.216 ± 0.019	0.23	-0.135 ± 0.020	1.2E-10
11[a]	[1.50,2.00)	[−2.7,−0.6)	1249	9.212 ± 0.005	0.19	53	9.276 ± 0.026	0.19	-0.064 ± 0.026	2.2E-02
12[a]	[2.00,4.75)	[−2.7,−0.6)	976	9.461 ± 0.007	0.23	24	9.523 ± 0.054	0.27	-0.062 ± 0.055	2.2E-01
13[a]	[0.09,1.00)	[−0.6, 1.4)	53	8.836 ± 0.017	0.12	10	8.886 ± 0.038	0.12	-0.051 ± 0.041	2.8E-01
14[a]	[1.00,1.50)	[−0.6, 1.4)	559	8.903 ± 0.007	0.16	49	8.989 ± 0.036	0.25	-0.086 ± 0.037	2.0E-02
15[a]	[1.50,2.00)	[−0.6, 1.4)	1726	9.018 ± 0.005	0.20	102	9.056 ± 0.022	0.23	-0.038 ± 0.023	8.9E-02
16[a]	[2.00,4.75)	[−0.6, 1.4)	1667	9.229 ± 0.007	0.29	131	9.183 ± 0.026	0.29	0.046 ± 0.027	7.0E-02

Notes. For each specified range, this table lists the number of optical and radio quasars N, and the (biweight) mean μ and (biweight) standard deviation σ for distributions of the logarithm of the BH mass. Both the difference of the means $\mu_O - \mu_R$ and the statistical chance the optical and radio quasars have the same mean as determined by the Student's T statistic P_T are listed.
[a]$\log M_{BH} > 8.7$ was also required.

higher to lower redshifts, and this trend characterizes both high and, to a somewhat lower degree, low-λ accreting BHs.

3.4 Mean accretion histories

The summary plots and tables discussed in Section 3.3, show that significant differences are present in the M_{BH}- and λ-distributions of optical and radio quasars. In this section, we go a step further and work out their relative expected accretion histories. To probe the average evolution of the radio and optical quasars of a given BH mass M_{BH}, we compute the BH mass function at any time via a continuity equation (e.g. Cavaliere, Morrison & Wood 1971; Small & Blandford 1992; Yu & Tremaine 2002; Marconi et al. 2004; Yu & Lu 2004; Hopkins, Richards & Hernquist 2007; Shankar, Bernardi & Haiman 2009b; Shankar et al. 2009c; Shankar 2009)

$$\frac{\partial n}{\partial t}(M_{BH}, t) = -\frac{\partial[\langle \dot{M}_{BH}\rangle n(M_{BH}, t)]}{\partial M_{BH}}, \tag{1}$$

where $\langle \dot{M}_{BH}\rangle = S(M_{BH}, z, \lambda)\langle\lambda\rangle M_{BH}/t_s$ is the mean accretion rate (averaged over the active and inactive populations, with $t_s = 4 \times 10^7(\epsilon/0.1)$ yr, with the radiative efficiency $\epsilon = 0.1$) of the optical BHs of mass M_{BH} at time t. Equation (1) states that the average growth rate of all BHs is proportional to the function $S(M_{BH}, z, \lambda)$, i.e. the fraction of BHs of mass M_{BH} active at redshift z and accreting at the Eddington rate λ. Equation (1) states that every BH, on average, constantly grows at the mean accretion rate $\langle \dot{M}_{BH}\rangle$ (see Steed & Weinberg 2003; Shankar et al. 2009c for further details). Note that we neglect any source term in equation (1), which may take into account the (uncertain) BH creation and merger rates. The latter is a reasonable assumption given that the overall local BH mass function can be easily accounted for assuming that most BHs grow through radiatively efficient accretion (see Shankar et al. 2009c).

Here, we further assume, for simplicity, that the function $S(M_{BH}, z, \lambda)$ can be further separated into

$$S(M_{BH}, z, \lambda) = p(\lambda, z)U(M_{BH}, z), \tag{2}$$

which imposes that all active BHs of mass M_{BH} at redshift z, share the same mean Eddington ratio distribution $p(\lambda, z)$, with $U(M_{BH}, z)$ the duty cycle, that is the *total* fraction of active BHs at redshift z and mass M_{BH} in the BH mass function $n(M_{BH}, z)$. We will further discuss the validity of this assumption. In models with a single value of λ, the duty cycle is simply the ratio of the luminosity and mass functions,

$$U(M_{BH}, z) = \frac{\Phi(L, z)}{\Phi_{BH}(M_{BH}, z)}, \qquad L = \lambda l M_{BH}, \tag{3}$$

with $l = 1.26 \times 10^{38}$ erg s^{-1} M$_\odot^{-1}$. A physically consistent model must have $U(M_{BH}, z) \leq 1$ for all M_{BH} at all times.

To model the mean accretion rate, we assume that optical and radio sources have a similar Gaussian shaped Eddington ratio distribution $p(\lambda, z)$, but with different means which evolve differently with time, as given by our results in the right-hand panel of Fig. 4. Unless otherwise noted, we assume that the standard deviation of the Gaussian Σ in λ is 0.7. Although, this value for Σ is slightly larger than what we actually observe, it accounts for some of the flux-limited biases discussed by Shen et al. (2008). We also note that the exact choice for Σ does not alter our results. We solve equation (1) using the numerical code discussed in Shankar et al. (2009c) and Shankar (2009), and we refer to those papers for full details. We briefly point out here that the code computes the total
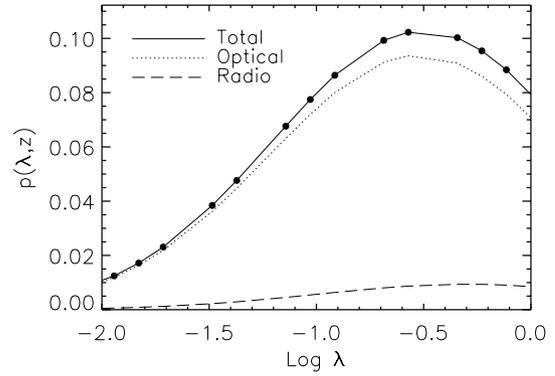
Figure 6. Eddington ratio distribution adopted in our modelling. The solid line shows the total Gaussian λ-distribution adopted for the full population of BHs. The solid points mark the actual discrete values of λ used in the computation. The dotted and long-dashed lines represent the separate distributions for optical and radio sources, respectively. We allow the peaks of the both Gaussian distributions to decrease in time following the different evolution for optical and radio sources shown in the right panel of Fig. 4.

duty cycle $U(M_{BH}, z)$ at any redshift z, given the BH mass function at redshift $z + dz$ and an input $p(\lambda, z)$ distribution. The code allows for any input $p(\lambda, z)$ distribution, as long as it is expressed in discrete form. Fig. 6 shows, for example, the Eddington ratio distribution adopted in our modelling at $z = 3$. The solid line shows the total λ-distribution adopted for the full BH population, while the solid circles mark the actual discrete values of λ used in the computation. The dotted and long-dashed lines represent the separate $p(\lambda, z)$ Gaussian distributions for optical and radio sources, respectively. We allow the median λ values peaks in the $p(\lambda, z)$ Gaussian distributions of optical and radio quasars, to decrease with decreasing redshift following the results in Fig. 4. The mean accretion rate then has two contributions represented by two terms

$$\langle \dot{M}_{BH}\rangle \propto \left[\int \lambda p_{opt}(\lambda, z)d\lambda + \int \lambda p_{radio}(\lambda, z)d\lambda\right] \times M_{BH} U(M_{BH}, z), \tag{4}$$

the first one $p_{opt}(\lambda, z)$ and the second one, $p_{radio}(\lambda, z)$, represented by the dotted and long-dashed lines in Fig. 6. We always assume $p_{radio} = 0.1 \times p_{opt}$, to satisfy the empirical constraint that radio sources are on average 10 per cent of the optical population (e.g. Jiang et al. 2007, and references therein). Note that we are here describing the radio population as a whole. It may well be true that compact and extended sources evolve differently along cosmic time but, as stated above, we leave this more subtle subdivision for a separate study.

Fig. 7 shows the mean accretion growth curves for BHs of different mass from $z = 4$ to 0. The mean BH mass at any time is computed from equation (1) by integrating the mean accretion rate,

$$M_{BH}(M_{BH,i}, z) = \int_{z_i}^{z} \langle \dot{M}_{BH}\rangle \frac{dt}{dz} dz. \tag{5}$$

The left-hand panel shows the curves of growth for radio sources alone, while the right-hand panel shows the optical ones. We find that, while optical quasars can grow up to a factor of 10 along the cosmic evolution from $z = 4$ to 0, despite having a higher Eddington ratio at $z > 2$, radio sources have an average growth not higher than a factor of ~2. This is due to their low duty cycle p_{radio}, roughly an order of magnitude lower than the optical one. Therefore, although radio sources do accrete at higher λ for a significant amount of time, their overall evolution is still much more moderate than the optical
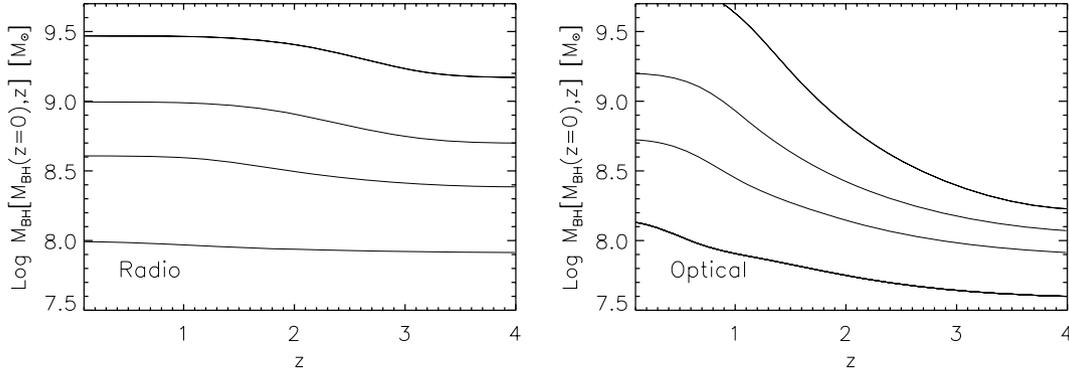
Figure 7. Mean accretion growth curves for BHs of different mass from $z = 4$ to 0. Left-hand panel: accretion histories for radio sources alone. Right-hand panel: accretion histories for the optical quasars (see text for further details). While radio sources only grow by a factor of ~ 2, at the most, optical quasars grow more and at later times.

one. The latter conclusion is strong against possible biases which might affect the exact value of the true underlying Eddington ratio distributions and their evolution with redshift.

Note that here we are not attempting to build a model for the whole, absolute evolution of all BHs, which would require a full match to the statistical and clustering properties of AGNs at all wavelengths (e.g. Shankar et al. 2008a; Shankar 2009, and references therein). Here, we are just interested to probe the *relative* growth of optical and radio quasars, and to this purpose we only adopt the optical quasar luminosity function by Richards et al. (2005, 2006a), which is *not* a complete representation of the overall AGN population (e.g. Hopkins et al. 2007; Shankar et al. 2009c, and references therein). Also, the adopted $p(\lambda, z)$ distributions are the ones described in Section 3.1, which may be affected by several biases and uncertainties (e.g. Shen et al. 2008). However, as long as radio and optical quasars are affected by similar selection effects (see Section 4), the relative comparison is physically meaningful.

We now show that we can efficiently test, for radio sources only, if our first assumption of having a mass independent underlying $p(\lambda, z)$ distribution is a reasonable one. It is clear that, knowing at each time-step the BH mass function from the continuity equation, and the mapping between (bolometric) luminosity L and BH mass $M_{\rm BH}$, provides directly the duty cycle $U(M_{\rm BH}, z)$ (see equation 3).

In other words, given the observed quasar or radio luminosity function $\Phi_x(L, z)$, the BH mass function $\Phi_{\rm BH}$, and the Eddington ratio distribution p_x, the duty cycle $U(M_{\rm BH}, z)$ can be derived by the equality (e.g. Steed & Weinberg 2003; Shankar 2009)

$$\Phi_x(L, z) = \int p_x(\log \lambda, z) U(M_{\rm BH}, z)$$
$$\times \Phi_{\rm BH}(M_{\rm BH}, z) d \log M_{\rm BH}, \tag{6}$$

with $x = $ opt or $x = $ radio. We apply equation (6) to infer the bolometric luminosity function of radio quasars, given the output duty cycle $U(M_{\rm BH}, z)$ and the underlying assumption that $p_{\rm radio} = 0.1 \times p_{\rm opt}$, constant for all BHs of any mass at any time. Fig. 8 shows the radio luminosity function predicted from equation (6) as solid lines at a (chosen) redshift of $z = 2.5$. The latter is compared with the grey area, which marks the luminosity function of radio sources in SDSS at the same redshift, obtained by correcting the quasar luminosity function from Richards et al. (2005) (long-dashed line in the same figure) by the luminosity and redshift-dependent radio fraction of optical sources inferred by Jiang et al. (2007). The left-hand panel shows the predictions assuming the $p_{\rm radio}(\lambda, z)$ distribution of radio sources in Fig. 6 to be constant with BH mass. It can be seen that the predictions overproduce the actual observed radio luminosity function at the faint end, which implies that the input $p(\lambda, z)$ is *not* correct. The right-hand panel of Fig. 8
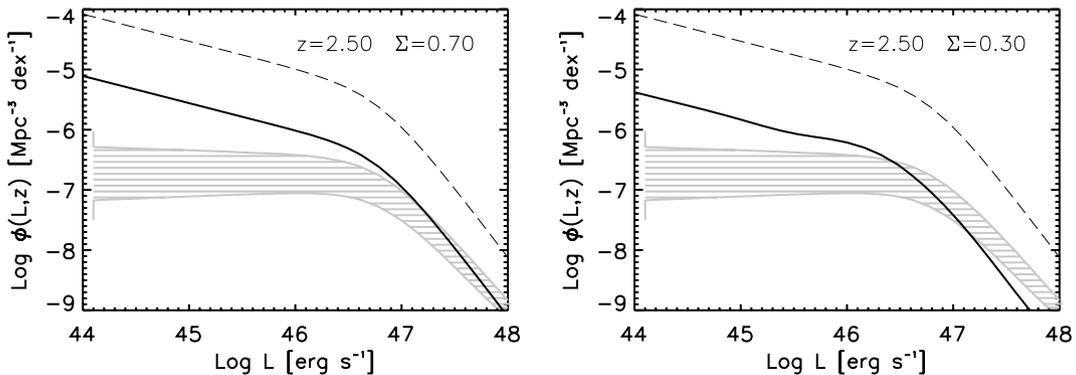
Figure 8. Solid lines in both panels are the predicted bolometric luminosity functions at $z = 2.5$ for radio sources alone, obtained by the convolution of the underlying total BH mass function with the assumed λ-distribution proper for radio sources (see text). The predicted luminosity functions are compared with grey areas that mark the optical luminosity function of radio sources alone in SDSS, expressed in bolometric units, obtained by correcting the optical quasar luminosity function from Richards et al. (2005; shown with long-dashed lines) by the fraction of radio-optical sources measured by Jiang et al. (2007) as a function of luminosity and redshift. Left-hand panel: shows the predictions assuming the intrinsic distribution of the $P(\lambda)$ distribution of radio sources is a Gaussian with dispersion $\Sigma = 0.7$ equal to the optical one. Right-hand panel: same as left-hand panel but assuming $\Sigma = 0.3$. Irrespective of the exact value for Σ, lower fractions of radio sources at lower BH masses are needed to reproduce the data.

shows the result of a similar exercise in which we instead insert a $p_{\text{radio}}(\lambda, z)$ distribution in the continuity equation with a much narrower intrinsic scatter of $\Sigma = 0.3$. The $z = 2.5$ predictions for the latter model imply now less radio sources at a given luminosity as the overall probability $p_{\text{radio}}(\lambda, z)$ is narrower, an effect which decreases the probability for BHs to be active as radio sources. However, it can be seen that even the latter model provides a poor match to the data. We conclude that, irrespective of the exact value for the broadness of the $p_{\text{radio}}(\lambda, z)$ distribution, the only way to reproduce the observed fraction of radio sources in the faint end of the quasar luminosity function, is to assume $p_{\text{radio}}(\lambda, z) = k(M_{\text{BH}})$ $p_{\text{opt}}(\lambda, z)$, with $k(M_{\text{BH}})$ being significantly lower than 10 per cent at lower BH masses. This would produce an increasingly lower fraction of BHs as active radio sources at lower masses, and a lower number of radio sources at fainter bolometric luminosities. These findings are in line with the results derived in local galaxies by Best et al. (2005), who claim a similar, or even steeper, decline of the AGN fraction with decreasing BH mass.

4 DISCUSSION

4.1 Looking for biases

The SDSS is flux-limited, and therefore one might argue that the possibly heavy loss of faint sources might bias our results on a different accretion history between optical and radio sources. However, Figs 2 and 3 show that even if we restrict our analysis to the subsample of BHs with mass $M_{\text{BH}} \gtrsim 10^9 \, \text{M}_\odot$, which always tend to shine above the SDSS flux limit (see Fig. 1), we find very similar Eddington ratio and BH mass distributions as in the total sample. In principle, massive BHs accreting at very low Eddington ratios should be missed in SDSS, thus possibly biasing the above result. However, we also note that the $z > 2$ median BH mass is $M_{\text{BH}} \sim 2 \times 10^9 \, \text{M}_\odot$ radiating at $\lambda \sim 0.4$, and SDSS would be able to detect them radiating down to $\lambda = 0.1$, that is $L_{\text{BOL}} \sim 2 \times 10^{46} \, \text{erg s}^{-1}$ (cf. Fig. 1).

Nevertheless, the results discussed in this paper may be significantly affected by other biases and measurement errors. For example, Shen et al. (2009) have recently discussed several selection biases which may underestimate the mean and broadness of the Eddington ratio distributions in flux limited samples. Also, the C IV lines may be affected by winds and therefore the masses of high-redshift quasars might be overestimated with respect to the Mg II based ones. Shen et al. (2009) discuss that C IV masses are correlated with the Mg II ones, although with a slight offset and much larger scatter. Analogously, the analysis of fluxes in the DR6 SDSS sample has shown that all fluxes may be systematically underestimated in the DR3 sample. Last but not least, even if reverberation mapping virial relations are (strongly) biased (e.g. Marconi et al. 2008, but see also Netzer 2009), this does not adversely affect our analysis or results. In fact, although all the above biases may induce strong uncertainties in the absolute measurements of BH masses or AGN bolometric luminosities, there is no obvious reason why they should affect radio and optical quasars in a different way. Therefore the relative, systematic offsets between radio and optical sources discussed in Section 3, should be reliable. Moreover, none of the effects listed above would be capable of inducing the *redshift-dependent* differences observed in the accretion histories of the two quasar populations.

A more subtle bias may arise from a different underlying mass distribution for optical and radio active BHs. In flux-limited samples, lower mass BHs with steeper number distribution are scattered into higher mass bins more efficiently than those in flatter number distribution, thus biasing the Eddington ratio distributions. For narrow Eddington ratio distributions and bright luminosities, the active BH mass function has a similar shape to the AGN luminosity function (see Shankar et al. 2009c), as also empirically found via direct calibration by Vestergaard et al. (2008). Therefore, a direct comparison of the optical and radio quasar luminosity function bright-end slopes, is similar to comparing the mass distributions of active BHs. To this purpose, we have multiplied the Richards et al. (2005) luminosity function for the usual, completeness-corrected radio fraction of Jiang et al. (2007) to yield an optical luminosity function for radio sources alone. We find that, at all redshifts of interest here, the bright-end slope for the radio-loud quasar luminosity function is always shallower than the optical one (note that the specific value of the bright-end slope of the quasar luminosity function is irrelevant for this test). This in turn would imply that BH masses for optical sources could be smaller and their intrinsic Eddington ratios higher. While this effect might play some role in the behaviour seen at $z < 2$, it would certainly not be able to explain the opposite behaviour seen at higher redshifts, where the effects due to the flux limits should be, if anything, even stronger.

A more physical bias may derive from the fact that our radio sampling is restricted to optically selected sources, and many more sources are found in high-frequency radio surveys which may not have counterparts in SDSS (e.g. Cirasuolo et al. 2003; de Zotti et al. 2005; Massardi 2008; De Zotti et al. 2009, and references therein). Nevertheless, although radio activity in AGNs is still not well understood and may pass through different stages (e.g. Croton et al. 2006; Blundell & Kuncic 2007; Heinz, Merloni & Schwab 2007; Cavaliere & Lapi 2008; Ghisellini & Tavecchio 2008; Merloni & Heinz 2008; Shankar et al. 2008c), it is clear that at least within luminous, optically selected sources, radio-loudness is not a simple function of BH mass or Eddington ratio, and that radio sources are not a mere random subsample of the optical ones.

4.2 Hints from clustering

We find that, since $z = 4$, the accretion histories of optical and radio source are significantly different, in a non-trivial and redshift-dependent way. This suggests that powerful radio and optical sources may be intrinsically different. Independent empirical studies on the clustering properties of optical and radio sources support our results. Negrello, Magliocchetti & De Zotti (2006) find that the observed two-point angular correlation function of milliJansky radio sources exhibits the puzzling feature of a power-law behaviour up to very large ($\sim 10°$) angular scales which cannot be accounted for in the standard hierarchical clustering scenario for any realistic redshift distribution of such sources. The radio sources responsible for the large-scale clustering signal are increasingly less clustered with increasing look-back time, up to at least $z \sim 1$, at variance with what found for optically selected quasars (e.g. Croom et al. 2005; Porciani & Norberg 2006). The data are accurately accounted for in terms of a bias function which decreases with increasing redshift, mirroring the evolution with cosmic time of the characteristic halo mass entering the non-linear regime. More recently, Shen et al. (2009) found that radio-loud quasars are more strongly clustered than radio-quiet quasars of similar mass. This implies that radio-loud quasars live in more massive dark matter haloes and denser environments than radio-quiet quasars, consistent with local $z < 0.3$ observations for radio-loud type 2 AGNs Mandelbaum et al. (2009) and radio galaxies (Lin et al. 2008; Wake et al. 2008). Also the

hosts of optical and radio quasars seem to have somewhat different structural properties (e.g. Wolf & Sheinis 2008).

4.3 Implications

The high BH mass, high-redshift radio sources observed in our sample might play a significant role in pre-heating the cores of groups and clusters (e.g. Bower, McCarthy & Benson 2008; Cavaliere & Lapi 2008; Merloni & Heinz 2008, and references therein). Completing their growth already at $z \gtrsim 2$, these massive BHs can in fact induce radiative and kinetic energy in their surroundings already at very early epochs, thus significantly contributing to increasing the entropy in their surroundings (e.g. Cavaliere & Lapi 2008). Moreover, if the radio AGN phenomenon is preferentially confined within the subsample of the optical quasars which tend to live in overdense environments (e.g. groups and clusters), the AGN radio feedback will prevent the ionization of lower density regions of the universe. This possibility might be reconciled with independent studies that find that any injection of non-gravitational energy in the diffuse baryons should avoid low-density regions at high redshift to be consistent with the void statistics of the $z \sim 2$ observed Lyman α forest (e.g. Borgani & Viel 2009).

It has been often discussed in the literature that a high BH mass may be a necessary although not sufficient, condition for AGN radio loudness (e.g. Laor 2000; Ho 2002; Best et al. 2005; Gopal-Krishna, Mangalam & Wiita 2008). A more recent study by Rafter, Crenshaw & Wiita (2009) suggests that, although there is indeed a tendency for the more massive BHs to have a higher probability of being active radio sources, no clear demarcation is apparent below a BH mass of $\sim 2 \times 10^8 \, M_\odot$. The results presented in Fig. 5 show that radio-loud quasars do actually cover a wide range of BH masses, and that their masses are offset with respect to those of optical quasars. More specifically, although radio-loud quasars are, on average, always characterized by higher BH masses, their offset with respect to optical quasars steadily decreases with increasing redshift, ending up at $z > 2$ having comparable, or even *lower*, BH masses than optical quasars. Our data therefore do not point to any clear trend between radio-loudness and specific BH mass. Instead, our analysis seems to suggest that radio and optical quasars have different accretion histories. While at most times radio-loud quasars are preferentially associated with more massive BHs than radio-quiet quasars, there is no clear dividing line in BH mass. However, as we show above from detailed evolutionary models, radio-loud quasars have not grown their mass by a significant amount since $z \sim 4$, mainly due to their low duty cycles. Thus, the massive radio-loud quasars observed at late times must have grown their mass at earlier epochs than those probed here (see also Overzier et al. 2009 for a similar conclusion on the rapid growth of $z > 4$ radio galaxies).

Several groups have also put forward the possibility of a similarity between X-ray/radio galactic binaries and AGNs (e.g. Meier 2001; Gallo, Fender & Pooley 2003; Maccarone, Gallo & Fender 2003; Merloni, Heinz & di Matteo 2003; Falcke, Körding & Markoff 2004; Fender, Belloni & Gallo 2004; Jester 2005). In particular, it has been shown that there might be a common scaling relation between X-ray luminosity, radio luminosity, and BH mass in X-ray binaries and AGNs (Merloni et al. 2003). Different observational states have been observed for X-ray binaries. In brief, X-ray sources at very low-Eddington ratios $\lesssim 10^{-2}$ are observed to be inefficient optical emitters, but efficient radio-jet emitters, and are therefore defined to be in a 'low (luminosity)/hard (spectrum)' (or power-law) state. At higher Eddington ratios, X-ray binaries are observed in a thermal, radiatively efficient, disc-dominated phase. When X-ray

binaries enter this thermal 'soft' state the steady jet is quenched (e.g. Gallo et al. 2003). A second transition occurs at Eddington ratios higher than 30 per cent when X-ray binaries enter a 'very high state' with a steep power-law spectrum and intermittent radio-jet activity. Given the similarities in accretion physics, it is tempting to associate similar states to AGNs. However, the results presented in Fig. 4 may pose serious problems to the connection between X-ray binaries and AGNs. In fact, radio sources in our sample encompass a significantly large range of Eddington ratios with no clear evidence of transition thresholds. Interestingly, Maoz (2007) also finds that a group of radio-loud low-ionization nuclear emission line regions (LINERs), which are thought to be radiatively inefficient sources with no 'big blue bump', shows instead a spectral energy distribution very similar to that of Seyfert galaxies, which require thin accretion discs. Also, several empirical works suggested (e.g. Churazov et al. 2001), also in analogy to X-ray binaries and microquasars (e.g. Reynolds & Begelman 1997; Nipoti, Blundell & Binney 2005), that radio activity might be a brief and 'intermittent' phase, tuned in a way to yield the low fraction of radio sources observed within optical samples. Although our study does not allow any definite constraint on such intermittency, it does however suggest that even if radio emission is intermittent, the cycles are not distributed randomly in time and mass.

Sikora et al. (2007) collected a significant sample of radio-loud and radio-quiet quasars, spanning a large range of Eddington ratios. They find that radio-loud sources define an upper sequence in the radio-loudness versus Eddington ratio plane, suggesting that there is no clear correlation between radio-loudness and BH mass or λ. Overall, we also find no significant connection between radio activity and BH mass and/or accretion rate, a result which may indicate, in agreement with Sikora et al. (2007), that other BH properties, such as the spin, may be responsible for the radio activity in some AGNs. In their analytic model, Wilson & Colbert (1995) were able to reproduce the radio luminosity function by assuming that radio-loud quasars are a different, non-random subsample of optical quasars characterized by a higher spin. More recently, Lagos, Padilla & Cora (2009) adopting a full model for galaxy and BH evolution, found that the final BH spin distribution depends almost exclusively on the BH accretion history, with the main mechanisms of BH spin-up being gas cooling processes and disc instabilities. They found that the more massive BHs, which are hosted by massive elliptical galaxies, have higher spin values than less-massive BHs, hosted by spiral galaxies. Similar results were also claimed by Volonteri, Sikora & Lasota (2007), who found that the observed radio loudness bimodality is directly related to the BH spin distribution in galaxies. In their model, BHs in giant elliptical galaxies are grown by merger-driven accretion and end up having, on average, much larger spins than BHs in spiral, disc galaxies.

5 CONCLUSIONS

In this paper, we have cross-correlated the SDSS DR3 sample with FIRST and with the Vestergaard et al. (2008) BH mass sample. We found significant statistical evidence for the radio sources to have a higher λ at $z > 2$ with respect to optical quasars. The situation reverses at $z < 1$, where radio sources have lower Eddington ratios. At $z > 2$, radio quasars tend to be less massive than optical quasars; however, as redshift decreases radio quasars happen to be in increasingly more massive BHs with respect to optical quasars. We have checked that all these results cannot be a result of any evident bias. For example, restricting to the subsample of active BHs with mass $\gtrsim 10^9 \, M_\odot$, which is not affected by flux-limited

effects, yields essentially equal results. Also, we have discussed that any other bias, such as systematic uncertainties in SDSS fluxes, in BH mass measurements or different slopes in the intrinsic active mass function of radio and optical quasars are not able to induce the *redshift-dependent* systematic differences we observe between radio and optical quasars in the SDSS data. Our results suggest that optical and optically selected radio sources have different accretion histories since very early epochs, and may be hosted by different dark matter haloes, as also suggested by some clustering measurements. We find no clear correlation between radio activity and BH mass and/or accretion rate in our data, which may hint towards another BH property as source of radio activity, such as the BH spin. We perform detailed modelling of the accretion histories of optical and radio sources in terms of a continuity equation and broad input Eddington ratio distributions. We find that while optical sources may grow up to an order of magnitude, radio sources had a much more contained growth since $z \sim 2$–4. The same modelling allows us to conclude that the probability for lower mass BHs to be radio loud must be lower than for higher mass BHs at all epochs, to reproduce the low fraction of radio sources at faint optical luminosities as observed in SDSS.

ACKNOWLEDGMENTS

REFERENCES

Allen S. W., Dunn R. J. H., Fabian A. C., Taylor G. B., Reynolds C. S., 2006, MNRAS, 372, 21
Becker R. H., White R. L., Helfand D. J., 1995, ApJ, 450, 559
Best P. N., Kauffmann G., Heckman T. M., Brinchmann J., Charlot S., Ivezić Ž., White S. D. M., 2005, MNRAS, 362, 25
Bird J., Martini P., Kaiser C., 2008, ApJ, 676, 147
Blandford R. D., 1999, in Merritt D. R., Valluri M., Sellwood J. A., eds, ASP Conf. Ser. Vol. 182, Galaxy Dynamics - A Rutgers Symposium. Astron. Soc. Pac., San Francisco, p. 87
Blandford R. D., Znajek R. L., 1977, MNRAS, 179, 433
Blandford R. D., Payne D. G., 1982, MNRAS, 199, 883
Blundell K. M., Kuncic Z., 2007, ApJ, 668, L103
Borgani S., Viel M., 2009, MNRAS, 392, 26
Bower R. G., McCarthy I. G., Benson A. J., 2008, MNRAS, 390, 1399
Cattaneo A., Best P. N., 2009, MNRAS, 395, 518
Cavaliere A., D'Elia V., 2002, ApJ, 571, 226
Cavaliere A., Lapi A., 2008, ApJ, 673, L5
Cavaliere A., Morrison P., Wood K., 1971, ApJ, 170, 223
Churazov E., Brüggen M., Kaiser C. R., Böhringer H., Forman W., 2001, ApJ, 554, 261
Churazov E., Sazonov S., Sunyaev R., Forman W., Jones G., Böhringer H., 2005, MNRAS, 363, 91
Ciotti L., Ostriker J. P., Proga D., 2009, ApJ, 699, 89
Cirasuolo M., Celotti A., Magliocchetti M., Danese L., 2003, MNRAS, 346, 447
Condon J. J., Cotton W. D., Greisen E. W., Yin Q. F., Perley R. A., Taylor G. B., Broderick J. J., 1998, AJ, 115, 1693
Croom S. M. et al., 2005, MNRAS, 356, 415
Croton D. J. et al., 2006, MNRAS, 365, 11
Dai X., Shankar F., Sivakoff G. R., 2008, ApJ, 672, 108
de Zotti G., Ricci R., Mesa D., Silva L., Mazzotta P., Toffolatti L., González-Nuevo J., 2005, A&A, 431, 893
De Zotti G., Massardi M., Negrello M., Wall J., 2009, A&A, in press (arXiv:0908.1896)
Dekel A. et al., 2009, Nat, 457, 451
Dietrich M., Mathur S., Grupe D., Komossa S., 2009, ApJ, 696, 1998
Falcke H., Körding E., Markoff S., 2004, A&A, 414, 895
Fanaroff B. L., Riley J. M., 1974, MNRAS, 167, 31P
Fender R. P., Belloni T. M., Gallo E., 2004, MNRAS, 355, 1105
Ferrarese L., Merritt D., 2000, ApJ, 539, L9
Fontanot F., Monaco P., Cristiani S., Tozzi P., 2006, MNRAS, 373, 1173
Gallo E., Fender R. P., Pooley G. G., 2003, MNRAS, 344, 60
Ganguly R., Brotherton M. S., Cales S., Scoggins B., Shang Z., Vestergaard M., 2007, ApJ, 665, 990
Gebhardt K. et al., 2000, ApJ, 539, L13
Ghisellini G., Tavecchio F., 2008, MNRAS, 387, 1669
Gopal-Krishna Mangalam A., Wiita P. J., 2008, ApJ, 680, L13
Graham A. W., 2007, MNRAS, 379, 711
Granato G. L., De Zotti G., Silva L., Bressan A., Danese L., 2004, ApJ, 600, 580
Granato G. L., Silva L., Lapi A., Shankar F., De Zotti G., Danese L., 2006, MNRAS, 368, L72
Hardcastle M. J., Evans D. A., Croston J. H., 2007, MNRAS, 376, 1849
Heinz S., Merloni A., Schwab J., 2007, ApJ, 658, L9
Hickox R. C. et al., 2009, ApJ, 696, 891
Ho L. C., 2002, ApJ, 564, 120
Hoaglin D. C., Mosteller F., Tukey J. W., 1983, Understanding Robust And Exploratory Data Analysis. Wiley Series in Probability and Mathematical Statistics. Wiley, New York
Hopkins P. F., Hernquist L., 2009, ApJ, 698, 1550
Hopkins P. F., Richards G. T., Hernquist L., 2007, ApJ, 654, 731
Jester S., 2005, ApJ, 625, 667
Jiang L., Fan X., Ivezić Ž., Richards G. T., Schneider D. P., Strauss M. A., Kelly B. C., 2007, ApJ, 656, 680
Kauffmann G., Heckman T. M., 2009, MNRAS, 397, 135
Keres D., Katz N., Fardal M., Dave R., Weinberg D. H., 2009, MNRAS, 395, 160
Kim M., Ho L. C., Peng C. Y., Barth A. J., Im M., Martini P., Nelson C. H., 2008, ApJ, 687, 767
Kollmeier J. A. et al., 2006, ApJ, 648, 128
Körding E. G., Jester S., Fender R., 2008, MNRAS, 383, 277
Lagos C. d. P., Padilla N. D., Cora S. A., 2009, MNRAS, 397, 31
Laor A., 2000, ApJ, 543, L111
Lapi A., Shankar F., Mao J., Granato G. L., Silva L., De Zotti G., Danese L., 2006, ApJ, 650, 42
Lazarian A., 2006, Astron. Nachr., 327, 609
Lin L. et al., 2008, ApJ, 681, 232
Liu Y., Jiang D.-R., 2006, Chin. J. Astron. Astrophys., 6, 655
Livio M., Ogilvie G. I., Pringle J. E., 1999, ApJ, 512, 100
Maccarone T. J., Gallo E., Fender R., 2003, MNRAS, 345, L19
McLure R. J., Dunlop J. S., 2004, MNRAS, 352, 1390
Mandelbaum R., Li C., Kauffmann G., White S. D. M., 2009, MNRAS, 393, 377
Maoz D., 2007, MNRAS, 377, 1696
Marchesini D., Celotti A., Ferrarese L., 2004, MNRAS, 351, 733
Marconi A., Hunt L. K., 2003, ApJ, 589, L21
Marconi A., Risaliti G., Gilli R., Hunt L. K., Maiolino R., Salvati M., 2004, MNRAS, 351, 169
Marconi A., Axon D. J., Maiolino R., Nagao T., Pastorini G., Pietrini P., Robinson A., Torricelli G., 2008, ApJ, 678, 693
Marulli F., Bonoli S., Branchini E., Moscardini L., Springel V., 2008, MNRAS, 385, 1846
Massardi M. et al., 2008, MNRAS, 384, 775
Meier D. L., 2001, ApJ, 548, L9
Meisenheimer K., 2003, New Astron. Rev., 47, 495

Menci N., Fiore F., Puccetti S., Cavaliere A., 2008, ApJ, 686, 219

Merloni A., Heinz S., 2008, MNRAS, 388, 1011

Merloni A., Heinz S., di Matteo T., 2003, MNRAS, 345, 1057

Metcalf R. B., Magliocchetti M., 2006, MNRAS, 365, 101

Miralda-Escudé J., Kollmeier J. A., 2005, ApJ, 619, 30

Monaco P., Fontanot F., 2005, MNRAS, 359, 283

Monaco P., Fontanot F., Taffoni G., 2007, MNRAS, 375, 1189

Murray N., Chiang J., Grossman S. A., Voit G. M., 1995, ApJ, 451, 498

Negrello M., Magliocchetti M., De Zotti G., 2006, MNRAS, 368, 935

Netzer H., Trakhtenbrot B., 2007, ApJ, 654, 754

Netzer H., Lira P., Trakhtenbrot B., Shemmer O., Cury I., 2007, ApJ, 671, 1256

Netzer H., 2009, ApJ, 695, 793

Nipoti C., Blundell K. M., Binney J., 2005, MNRAS, 361, 633

Overzier R. A. et al., 2009, ApJ, 704, 548

Pipino A., Silk J., Matteucci F., 2009, MNRAS, 392, 475

Porciani C., Norberg P., 2006, MNRAS, 371, 1824

Rafter S. E., Crenshaw D. M., Wiita P. J., 2009, AJ, 137, 42

Rawlings S., Saunders R., 1991, Nat, 349, 138

Rees M. J., 1984, ARA&A, 22, 471

Reynolds C. S., Begelman M. C., 1997, ApJ, 487, L135

Richards G. T. et al., 2005, MNRAS, 360, 839

Richards G. T. et al., 2006a, AJ, 131, 2766

Richards G. T. et al., 2006b, ApJS, 166, 470

Saxton C. J., Bicknell G. V., Sutherland R. S., Midgley S., 2005, MNRAS, 359, 781

Sazonov S. Y., Ostriker J. P., Ciotti L., Sunyaev R. A., 2005, MNRAS, 358, 168

Schneider D. P. et al., 2005, AJ, 130, 367

Shankar F., 2009, New Astron. Rev., 53, 57

Shankar F., Salucci P., Granato G. L., De Zotti G., Danese L., 2004, MNRAS, 354, 1020

Shankar F., Lapi A., Salucci P., De Zotti G., Danese L., 2006, ApJ, 643, 14

Shankar F., Crocce M., Miralda-Escude' J., Fosalba P., Weinberg D. H., 2008a, ApJ, submitted (arXiv:0810.4919)

Shankar F., Dai X., Sivakoff G. R., 2008b, ApJ, 687, 859

Shankar F., Cavaliere A., Cirasuolo M., Maraschi L., 2008c, ApJ, 676, 131

Shankar F., Sivakoff G. R., Vestergaard M., Bird J., Dai X., 2009a, MNRAS, submitted

Shankar F., Bernardi M., Haiman Z., 2009b, ApJ, 694, 867

Shankar F., Weinberg D. H., Miralda-Escudé J., 2009c, ApJ, 690, 20

Shen Y., Greene J. E., Strauss M. A., Richards G. T., Schneider D. P., 2008, ApJ, 680, 169

Shen Y. et al., 2009, ApJ, 697, 1656

Silk J., 2005, MNRAS, 364, 1337

Sikora M., Stawarz Ł., Lasota J.-P., 2007, ApJ, 658, 815

Small T. A., Blandford R. D., 1992, MNRAS, 259, 725

Steed A., Weinberg D. H., 2003, ApJ, submitted (astro-ph/0311312)

Trump J. R. et al., 2006, ApJS, 165, 1

Vestergaard M., 2004, ApJ, 601, 676

Vestergaard M., Fan X., Tremonti C. A., Osmer P. S., Richards G. T., 2008, ApJ, 674, L1

Vittorini V., Shankar F., Cavaliere A., 2005, MNRAS, 363, 1376

Volonteri M., Sikora M., Lasota J.-P., 2007, ApJ, 667, 704

Wake D. A. et al., 2008, MNRAS, 387, 1045

Willott C. J., Rawlings S., Blundell K. M., Lacy M., 1999, MNRAS, 309, 1017

Wilson A. S., Colbert E. J. M., 1995, ApJ, 438, 62

Wolf M. J., Sheinis A. I., 2008, AJ, 136, 1587

Yu Q., Lu Y., 2004, ApJ, 602, 603

Yu Q., Lu Y., 2008, ApJ, 689, 732

Yu Q., Tremaine S., 2002, MNRAS, 335, 965

This paper has been typeset from a TEX/LATEX file prepared by the author.